Journal of Engineering Science and Technology
Vol. 6, No. 5 (2011) 586 - 605
© School of Engineering, Taylor's University

BATCH STUDY, EQUILIBIRUM AND KINETICS OF ADSORPTION OF SELENIUM USING RICE HUSK ASH (RHA)

CH. SEKHARARAO GULIPALLI[1], B. PRASAD[1], KAILAS L. WASEWAR[2,*]

[1]Department of Chemical Engineering, Indian Institute of Technology (IIT) Roorkee – 247667, Uttarakhand, India
[2] Department of Chemical Engineering, Visveswarya National Institute of Technology (VNIT) Nagpur - 440010, Maharashtra, India
*Corresponding Author: k_wasewar@rediffmail.com

Abstract

The present work involves the study of Se(IV) adsorption onto rice husk ash (RHA). The adsorbents were coated with the ferric chloride solution for the effective removal of selenium. The physico-chemical characterization of the adsorbents was carried out using standard methods, e.g., proximate analysis, scanning electron microscopy (SEM), fourier transform infrared spectroscopy (FTIR), thermo-gravimetric (TGA) and differential thermal analysis (DTA), etc. Batch experiments were carried out to determine the effect of various factors such as adsorbent dose (w), initial pH, contact time (t), and temperature (T) on adsorption process. Se(IV) adsorption is high at low pH values, and decreased with the rise in initial pH. Temperature study shows that the uptake of Se(IV) is more at 293 K within the temperature range studied. The parameters of Pseudo-First order, Pseudo-Second order kinetics, Weber-Morris intra particle kinetics have been determined. Equilibrium isotherms have been analyzed using Langmuir isotherm, Freundlich isotherm and Temkin isotherm. Error analysis has also been done using hybrid fractional error function (HYBRID) and Marquardt's percent standard deviation (MPSD).

Keywords: Adsorption, Selenium, Rice Husk Ash (RHS), Equilibrium, Kinetics, Batch study, Thermal degradation.

1. Introduction

In India several incidents of chronic selenium toxicity in animals have been reported. Selenium poisoning in domestic buffaloes in the Karnal area of the North West plain of India has been reported. High selenium levels found in the animals are attributed to

Nomenclatures

B_T	Temkin Isotherm constant, related to the heat of adsorption
B	Temkin Isotherm constant
C_e	Equilibrium liquid phase concentration, µg/l
C_o	Initial concentration of adsorbate in solution, µg/l
C_t	Equilibrium liquid phase concentration after time t, µg/l
h	Initial sorption rate, µg/g.min
i	Constant that gives idea about the thickness of boundary layer, µg/g
K_F	Freundlich constant, l/µg
K_{id}	Intra-particle diffusion rate constant, µg/g $min^{1/2}$
K_L	Langmuir adsorption constant, l/µg
k	Rate constant, min^{-1}
k_f	Pseudo 1st order rate constant, min^{-1}
k_s	Pseudo-second-order rate constant, g/µg.min
$1/n$	Mono-component (non-competitive), Freundlich heterogeneity factor of the single component, dimensionless
q_e	Equilibrium adsorption capacity, µg/g
q_t	Equilibrium adsorption capacity after time t, µg/g
R	Universal gas constant, 8.314 J/mol K for air
R^2	Correlation coefficients
T_{max}	DTG peak temperature, K
T_{1i}	DTA first initial temperature, K
T_{2f}	DTA second final temperature, K
t	Time, min.
V	Volume of the solution, l
w	Mass of the adsorbent, g/l

Abbreviations

CPCB	Central pollution control board
DTA	Differential thermal analysis
DTG	Differential thermal gravimetery
EDAX	Energy dispersive X-ray analysis
FTIR	Fourier transform infrared spectroscopy
HYBRID	Hybrid fractional error function
ICPMS	Inductively coupled plasma mass spectroscopy
MPSD	Marquardt's percent standard deviation
RHA	Rice husk ash
SEM	Scanning electron microscopy
TG	Thermal gravimetery
TGA	Thermo-gravimetric analysis
UNICEF	United nations international children's emergency fund
US EPA	United States Environmental Protection Agency

the readily available selenium in the alkaline soils of the regions. Selenium is leached from the soil by irrigation water in the paddy fields and is taken up by rice plants, which accumulates it to toxic levels in the straw. This is the main fodder of the animals after harvest and is immediate cause of the toxicity. A similar pattern of mobilization of naturally occurring selenium caused by paddy

field irrigation that also resulted in poisoning of domestic animals was reported from southern India [1].

The typical concentration of selenium in wastewater is always more than the 0.05 mg/l and generally around 0.1 mg/l. Because of its high toxicity, the US EPA has proposed a standard of 0.05 mg/l for drinking water. For inland surface water, public sewers and marine/coastal areas, the Central Pollution Control Board (CPCB), Delhi, India has set a standard of 0.05 mg/l [2].

A lot of work on the adsorption of heavy metals and other toxic compounds are available [3-31]. There are several methods available for removal of selenium from water in large conventional treatment plants. These include adsorption by ferrihydrite, catalyzed cementation, biological reduction, enzymatic reduction etc. For high strength and low volumes of wastewater, heavy metal removal by adsorption technique is good proposition. A various studies of adsorption of selenium from water and wastewaters using various adsorbents have been summarized in Table 1.

In view of environmental aspects, it is essential to remove the selenium to desired concentration from wastewater. In present paper, investigation has been carried out to study the removal of selenium from aqueous phase by adsorption using rice husk ash (RHA). Characterizations of RHA, batch study, equilibrium, kinetics, thermodynamic, and thermal degradation were carried out. Also the error analysis was reported to select the best isotherm.

2. Materials and Methods

2.1. Materials

Adsorbents

Adsorption of Se(IV) was studied using rice husk ash (RHA). RHA were obtained from Bhawani Paper Mills, Raebareli, U.P. India. Adsorbents was washed with 0.1M $FeCl_3$ solution for effective removal of any Se(IV). After washing, they were dried in an oven at $105^{O}C$ for 72 h. This time was sufficient to drive off the moisture. After drying, adsorbents were stored in sealed glass bottles until use.

Adsorbates

All the chemicals used in the study were of laboratory grade reagent (LR) grade, Sodium selenite (Na_2SeO_3) has been taken as source of Se(IV) and this was supplied by Hi-Media Research Laboratory, Mumbai, India. The required quantity of the adsorbate was accurately weighed and dissolved in a small amount of distilled water and subsequently made up to 1 litre in a measuring flask by adding distilled water.

Other Chemicals

All other chemicals used in the study viz., acids, alkalies, $FeCl_3$, KBr, etc were supplied by S.D. Fine Chemicals, Mumbai, India.

Table 1. Batch Studies on Removal of Selenium by Various Adsorbents.

Adsorbents / Adsorbates	Conclusions	Ref.
Sulphuric acid-treated peanut shell Se(IV)	Se(IV) removal rate was found slower for the dry sorbent than for the wet sorbent with removal data fitting well a pseudo-first-order model. Sorption of Se(IV) follows the Langmuir equation with an increase in uptake as temperature rises due to an expected increase in the swelling of the sorbent allowing more active sites to become available for metal ions.	[3]
Iron oxides Se(IV), Se(VI)	The sorption follows a pseudo-second order kinetics.Variation of the sorption onto goethite with the selenium concentration in solution has been modelled considering a Langmuir isotherm. The main trend of the variation of the selenium sorption with pH is an increase at acidic pH.	[4]
Modified rice husk Cd(II) , Se(IV)	Kinetics data for both metals were found to follow pseudo-second order model. Cd(II) sorption was low at low pH values and increased with pH increase, however, Se(IV) sorption was high at low pH values, and decreased with the rise in initial pH until pH 7.	[5]
Hydrous aluminum oxide (HAO) and corundum (α-Al2O3) Se(IV), Se(VI)	The results t highlight the fact that adsorption mechanisms of oxyanions on mineral surfaces are strongly influenced by sorbent surface properties. The results are also generally consistent with a structure-based reactivity for metal oxides.	[6]
Cs-covered Si(100) 2 x 1 surfaces Se(IV), Se(VI)	Adsorption of Se on Cs/Si(100) surface system results in Se being initially adsorbed on sites different than that occupied by Cs up to 0.5 ml of Se deposition and forms SiSe compound. Higher Se deposition leads to a strong Cs–Se and Si–Cs–Se interaction, which leads to a disorder of the surface. The CsSe and Si–Se–Cs compounds are removed from the surface at about 1050 K.	[7]
Mg–Al and Zn–Al layered double hydroxides Se(IV), Se(VI)	Experiments examining the removal of SeO32- and SeO42- from aqueous solutions by LDHs indicated that the SeO32- and SeO42- could be adsorbed on Mg–Al and Zn–Al LDHs. Adsorption isotherms could be fitted according to the Langmuir equation.	[8]
Ferrihydrite Se(VI)	Se(VI) is removed from the water at pH below 4	[9]
GaAs(111)A–(2x2)surface Se(VI)	The Se-induced R300 reconstruction is formed in the very narrow ranges of temperature and Se coverage. For the GaAs (111) A–R300 Se surface structure model consisting of two Se trimer and three Ga vacancies per unit cell are proposed. and have determined the atomic coordinates: the trimer has a Se–Se bond length of 2.68 A and is adsorbed at the H site of the GaAs (111)A 3 surface.	[10]
Acidic and alkaline soils Se(IV), Se(VI)	Adsorptionrdesorption behavior of Se was investigated in laboratory studies for surface soil samples varying in physico-chemical characteristics and mineralogical composition. In general, greater amount of Se was sorbed by acidic soils than alkaline soils; the only exception was the alkaline seleniferous soil from Barwa in northwestern India. Adsorption data for Se fitted well to Freundlich isotherm	[11]
Aluminum-Oxide-Coated sand (AOCS) Se(IV), Se(VI)	The results reveal that the adsorption rate of Se(IV) increases more rapidly than that of Se(VI) in the initial period and both of them reach meta stable equilibrium with in 60 mins. The adsorption of Se(IV) onto AOCS surface is higher than that for Se(VI) under the same system pH (3-12)	[12]
Iron oxyhydroxide and manganese dioxide Se(IV), Se(VI)	The results show that the amorphous iron oxyhydroxide adsorbs more selenate and selenite than manganese dioxide at a given pH and site concentration. Selenite adsorbs more strongly than selenate on both oxides and selenate does not adsorb on manganese dioxide. Selenium adsorption decreases with increasing pH and decreasing particle concentration.	[13]

2.2. Methods

Adsorbent Characterization

The characteristics of the adsorbents were carried out by using standard procedure of proximate analysis, particle size analysis, scanning electron microscopic (SEM) analysis, energy dispersive X-ray (EDAX) analysis, Fourier transform infra red (FTIR) spectral analysis. The detail procedure is same as used by Wasewar et al. [14].

Batch Study

A water-bath temperature controlled shaker (Remi Instruments, Mumbai, India) was used for the batch adsorption study. The temperature range of 293 K to 323 K was used for Se(IV) adsorption. The batch experiments were performed at the constant shaking speed. For each experimental run, 50 ml aqueous solution of the known concentration of Se(IV) was taken in a 150 ml conical flask containing a known mass of the adsorbent. These flasks were agitated at a constant shaking rate of 150 rpm in a temperature controlled orbital shaker maintained at a constant temperature. Batch adsorption experiments were conducted for the removal of Selenium from water by $FeCl_3$ coated adsorbent. The effect of various parameters, adsorbent dose, w, initial pH (pH_o), contact time, t, initial concentration, C_o, and temperature on the adsorption of Se(IV) onto $FeCl_3$ coated RHA were presented.

Kinetic Study

To determine the necessary time for adsorption, 50 ml of the aqueous solution containing 100 μg/L of the specific Se(IV) was taken in a series of conical flasks. Known amount of the adsorbent was added to different flasks. The flasks were kept in shaker and the aqueous solution-adsorbent mixtures were stirred at constant speed. At the end of the predetermined time, t, the flasks were withdrawn, their contents were centrifuged, and the supernatant analyzed for adsorbate concentration. Adsorption kinetics was followed for 3 h and it was observed that after 1 h, there was gradual but very slow removal of the Se(IV) from the solution. In order to investigate the kinetics of adsorption of the Se(IV) on RHA, various kinetic models, like pseudo-first-order [15], pseudo-second-order [16] and intra-particle diffusion [17] models have been used.

The pseudo-second-order model can be represented in the following form

$$\log(q_e - q_t) = \log q_e - \frac{k_f}{2.303} t \tag{1}$$

This equation is, however, valid only for the initial period of adsorption. Various investigators have erroneously fitted this equation to the adsorbate uptake data for later periods, ignoring the data of the initial period for the model fitting.

The pseudo-second-order model can be represented in the following form:

$$q_t = \frac{ht}{1 + k_s q_e t} \tag{2}$$

where

$$h = k_S q_e^2 \tag{3}$$

The adsorbate transport from the solution phase to the surface of the adsorbent particles occurs in several steps, The overall adsorption process may be controlled either by one or more steps, e.g., film or external diffusion, pore diffusion, surface diffusion and adsorption on the pore surface, or a combination of more than one step. In a rapidly stirred batch adsorption, the diffusive mass transfer can be related by an apparent diffusion coefficient, which will fit the experimental sorption-rate data. The possibility of intra-particle diffusion was explored by using the intra-particle diffusion model:

$$q_t = k_{id}\sqrt{t} + I \tag{4}$$

where k_{id} is the intra-particle diffusion rate constant (μg/g min$^{1/2}$) and I (μg/g) is a constant that gives idea about the thickness of the boundary layer, i.e., larger the value of I, the greater is the boundary layer effect.

If the Weber-Morris plot of q_t versus $\sqrt{t}$ satisfies the linear relationship with the experimental data, then the sorption process is found to be controlled by intra-particle diffusion only. However, if the data exhibit multi-linear plots, then two or more steps influence the sorption process.

The mathematical dependence of fractional uptake of adsorbate on $\sqrt{t}$ is obtained if the sorption process is considered to be influenced by diffusion in the cylindrical (or spherical) and convective diffusion in the adsorbate solution. It is assumed that the external resistance to mass transfer surrounding the particles is significant only in the early stages of adsorption. This is represented by the first sharper portion. The second linear portion is the gradual adsorption stage with intra-particle diffusion dominating.

Equilibrium Study

For adsorption isotherms, experiments were carried out at natural pH_o of the samples by contacting a fixed amount of adsorbent (0.2 g) with 50 mL of Se(IV) solutions having C_o in the range of 100-500 μg/L. The mixture was centrifuged until equilibrium was attained and Se(IV) concentration in the supernatant solution and in the adsorbent was estimated.

Three two-parameter models; Langmuir, Freundlich, and Temkin have been used to correlate the experimental equilibrium adsorption data. The experimental equilibrium adsorption data of Se(IV) adsorption onto $FeCl_3$ coated RHA have been tested by using the two-parameter Freundlich [18], Langmuir [19], and Tempkin [20] isotherm equations.

Freundlich [18]

$$q_e = K_F C_e^{1/n} \tag{5}$$

Langmuir [19]

$$q_e = \frac{q_m K_L C_e}{1 + K_L C_e} \tag{6}$$

Tempkin [20]

$$q_e = B_T \ln K_T + B_T \ln C_e \tag{7}$$

The Freundlich isotherm is valid for a heterogeneous adsorbent surface with a non-uniform distribution of heat of adsorption over the surface. The Langmuir

isotherm, however, assumes that the sorption takes place at specific homogeneous sites within the adsorbent.

Error Analysis

Two error functions of non-linear regression basis were employed in this study to find out the most suitable kinetic and isotherm models to represent the experimental data respectively. The hybrid fractional error function (HYBRID) and the Marquardt's percent standard deviation (MPSD) error function [21, 22]. These error functions are given as

$$\text{HYBRID} = \frac{100}{n-p}\sum_{i=1}^{n}\left[\frac{(q_{e,\exp} - q_{e,calc})}{q_{e,\exp}}\right]_i \tag{8}$$

$$\text{MPSD} = 100\sqrt{\frac{1}{n-p}\sum_{i=1}^{n}\left(\frac{(q_{e,\exp} - q_{e,calc})}{q_{e,\exp}}\right)_i^2} \tag{9}$$

HYBRID was developed to improve the fit of the square of errors function at low concentration values. The MPSD is similar in some respects to a geometric mean error distribution modified according to the number of degrees of freedom of the system.

Thermal Analysis of Spent Adsorbents

The spent adsorbents obtained as a result of adsorption of Se(IV) were characterized by FTIR, SEM, TGA, and DTA analyses techniques. The thermal degradation (gasification) characteristics of the blank and spent adsorbents were studied using the thermo-gravimetric and differential analysis techniques. The thermal degradation of the adsorbents was carried out non-isothermally at the Institute Instrumentation Centre, IIT, Roorkee using the TGA analyzer from Perkin Elmer, Pyris Diamond.

In the present study, the operating pressure was kept slightly positive. The samples were prepared carefully after crushing and sieving so as to obtain homogeneous material properties. The sample was uniformly spread over the crucible base in all the experiments and the quantity of sample taken was 5-10 mg in all the runs. The oxidation runs were taken at heating rate of 25 K/min under an oxidizing atmosphere (flowing moisture-free air) for gasification. The tests were conducted over a range of temperature from the ambient temperature to 1000 ^{0}C. Flow rate of nitrogen/air was maintained at 200 ml/min.

The weight loss, during thermal heating was continuously recorded and downloaded using the software, Muse, Pyris Diamond. The instrument also provided the continuous recording of the differential thermal gravimetry (DTG) and differential thermal analysis (DTA) as a function of sample temperature and time. The TG, DTG and DTA curves obtained in each case were analyzed to understand the behavior of thermal degradation.

Few experiments were repeated to find the consistency in the results and it was found within ±2%.

3. Results and Discussion

3.1. Characterization of Adsorbents

RHA were treated with 0.1M $FeCl_3$ solution. The physico-chemical characteristics of the adsorbents such as proximate analysis carried out. The energy dispersive X-ray (EDAX) analysis, scanning electron microscopy (SEM) analyses and Fourier transform infra red (FTIR) spectral analysis were used to study the structural and morphological characteristics of adsorbents.

Physico-chemical Characterization of Adsorbents

Proximate analysis and particle size of the RHA are presented in Table 2. The SEM micrographs of $FeCl_3$ coated adsorbents and Se(IV) loaded adsorbents are shown in Fig. 1. It shows surface texture and porosity of the blank and loaded adsorbents. It can be inferred from these figures that the surface texture of the blank adsorbents changes drastically after the loading of the adsorbates.

Table 2. Proximate Analysis of RHA.

Characteristics	Value
Moisture (%)	10.07
Volatile matter (%)	15.03
Ash (%)	69.61
Fixed Carbon (%)	5.36
Average particle size (μm)	412

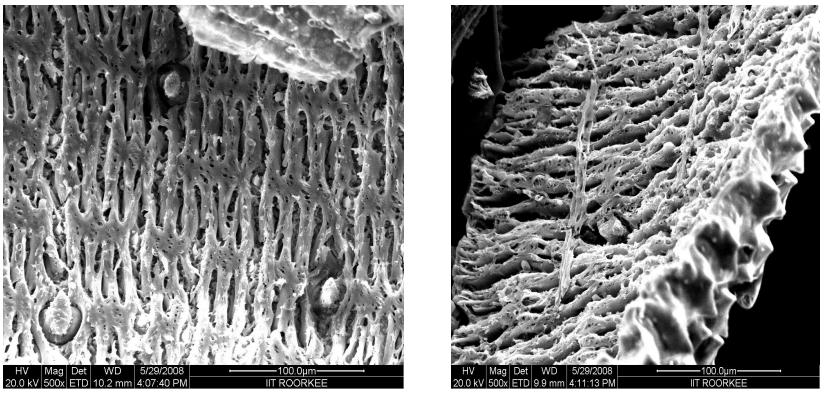

(a) **(b)**

Fig. 1. SEM Micrographs of (a) Blank and (b) Se(IV) Loaded RHA at 500X.

Energy dispersive X-ray analysis (EDAX) analysis of the adsorbent before and after adsorption was performed to estimate the composition of various elements present in the adsorbents. EDAX spectra indicates presence of elemental selenium after adsorption onto adsorbent as shown in Fig. 2. It indicates that at the adsorbent surface Se(IV) was reduced to elemental selenium.

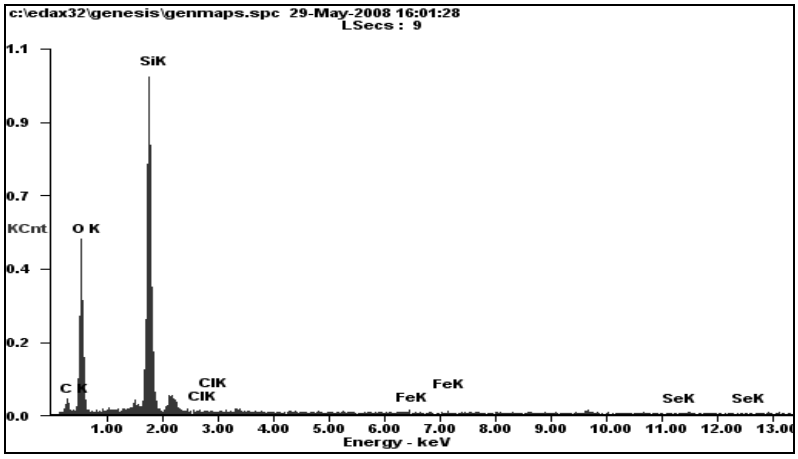

(a)

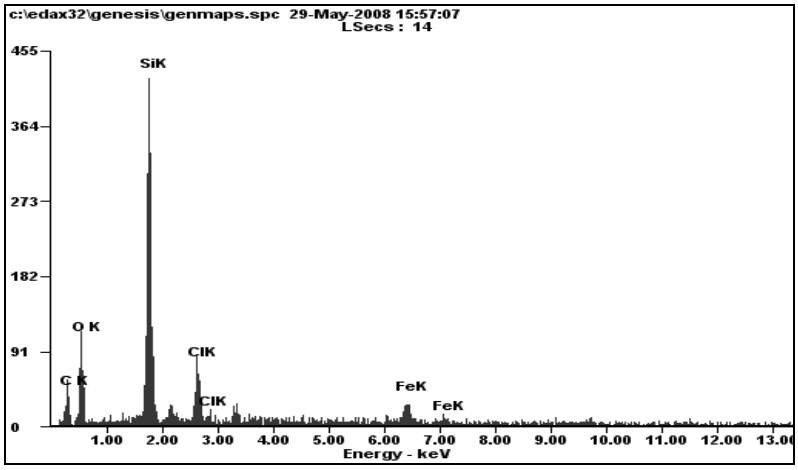

(b)

Fig. 2. EDAX Analysis of (a) Blank and (b) Se(IV) Loaded RHA.

The chemical structure of the adsorbents is of vital importance in understanding the sorption process. The adsorption capacity of adsorbents is strongly influenced by the chemical structure of their surface. The carbon-oxygen functional groups are by far the most important structures that influence the surface characteristics and surface behavior of adsorbents. The functional groups suggested most often are (I) carboxyl groups, (II) phenolic hydroxyl groups, (III) carbonyl groups (e.g., quinone-type), and (IV) lactone groups (e.g., fluorescein-type) The FTIR technique is an important tool to identify the characteristic functional groups, which are instrumental in adsorption of Se(IV). The FTIR spectra of the $FeCl_3$ coated and Se(IV)-loaded RHA is shown in Fig. 3.

A broad band between 3100 and 3700 cm^{-1} in all the adsorbents is indicative of the presence of both free and hydrogen bonded OH groups on the adsorbent surface. This stretching is due to both the silanol groups (Si-OH) and adsorbed water (peak at 3400 cm^{-1}) on the surface. C-O group stretching from aldehydes

and ketones can also be inferred from peaks in the region of 1600 cm^{-1}. These FTIR spectra also show transmittance around ~1100 cm^{-1} region due to the vibration of the CO group in lactones and due to Si-O-Si and –C-OH stretching and –OH deformation.

Figure 3 shows bands appearing at 3451 and 3457 cm^{-1} in spectra of RHA indicate presence of O-H bonding. C=C stretching indicates presence of bands at 1633 cm^{-1}. Although some inference can be drawn about the surface functional groups participating in the adsorption process from FTIR spectra, the weak and broad bands do not provide any authentic information about the nature of the surface oxides.

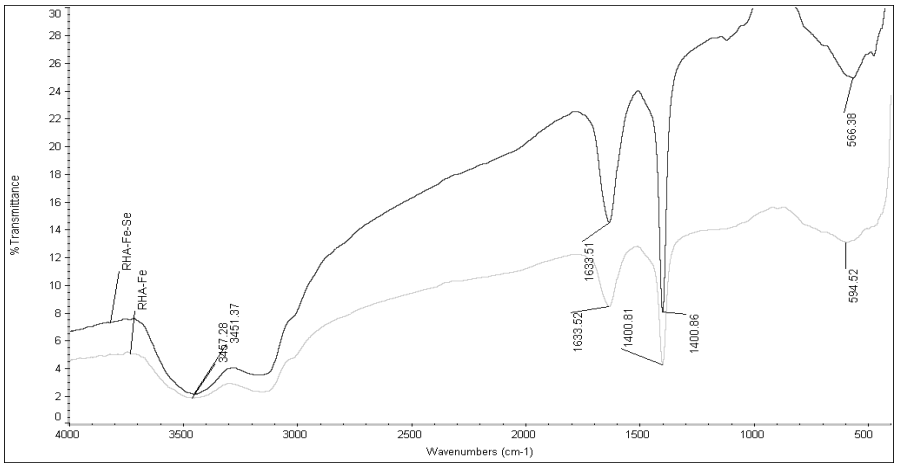

Fig. 3. FTIR Spectra of RHA and Se(IV)-Loaded RHA.

3.2. Batch Study

Batch adsorption experiments were conducted for the removal of Selenium from water by $FeCl_3$ coated RHA. Evaluation of various parameters, adsorbent dose, *w*, initial pH (pH_o), contact time, *t*, initial concentration, C_o, and temperature is of vital importance in the design of any adsorption system for the removal of Se(IV). The effect of these parameters on the adsorption of Se(IV) onto $FeCl_3$ coated RHA are presented.

Effect of Adsorbent Dosage (*w*)

The effect of w on the uptake of Se(IV) onto $FeCl_3$ coated RHA was studied for C_o = 100 µg/l and is shown in Fig. 4. The optimum adsorbent dosage *w* was found to be 6 g/l. It was found that the removal of Se(IV) by any of the adsorbents increases with an increase in the adsorbent dosage initially and, thereafter, becomes constant after some value of *w*. This value is taken as the optimum dosage *w*.

The increase in adsorption with the adsorbent dosage can be attributed to the availability of greater surface area and larger number of adsorption sites. At $w < w_{optimumu}$, the adsorbent surface becomes saturated with Se(IV) and the residual

Se(IV) concentration in the solution is large. With an increase in w, the Se(IV) removal increases due to increased Se(IV) uptake by the increased amount of adsorbent. For $w < w_{optimumu}$, the incremental removal of Se(IV) becomes very small as the surface Se(IV) concentration and the solution Se(IV) concentration come to near equilibrium with each other. At about $w < w_{optimumu}$, the removal efficiency becomes almost constant for the removal of Se(IV) onto $FeCl_3$ coated RHA.

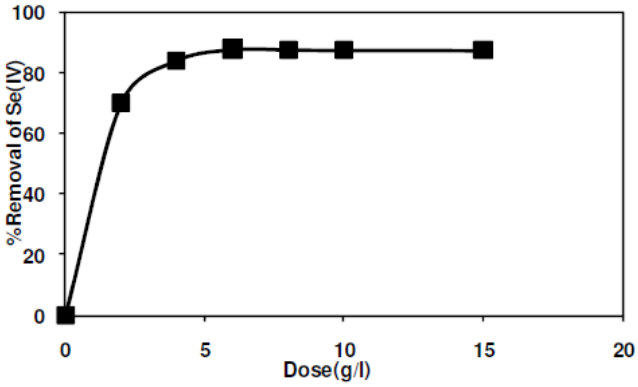

Fig. 4. Effect of Adsorbent Dose on the Removal of Se by RHA. T=303 K, t = 3 h, C_o=100 µg/l.

Effect of Contact Time

The effect of contact time on the removal of Se(IV) onto $FeCl_3$ coated RHA is shown in Fig. 5. The rate of removal of Se(IV) from water is very fast with all the adsorbents. This is obvious from the fact that a large number of vacant surface sites are available for the adsorption during the initial stage and with the passage of time, the remaining vacant surface sites are difficult to be occupied due to repulsive forces between the solute molecules on the solid phase and in the bulk liquid phase.

The adsorption of Se(IV) remains almost constant and the difference between the adsorptive uptake at 2 h and 3 h and is less than 1% of that at 5 h. Therefore, a steady-state approximation was assumed and a quasi-equilibrium situation was considered at t = 2 h. pH was not adjusted during the experiments. Based on these results kinetic studies, viz. pseudo first order, psedo second order, weber moris are perfomed on all Se(IV) adsorbent systems.

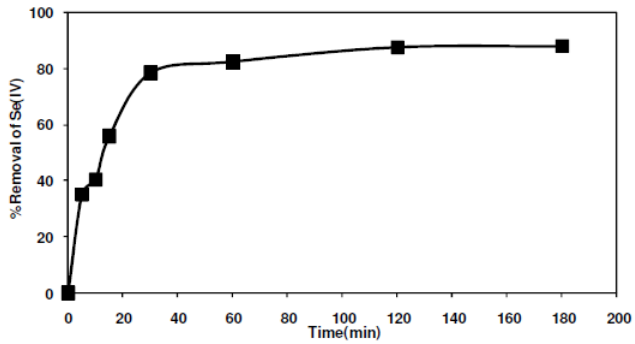

Fig. 5. Effect of Contact Time on % Removal of Se(IV) by RHA. T=303 K, C_o=100 µg/l.

Effect of pH

The pH_o of the aqueous solution with C_o = 100 µg/l of Se(IV) is found to be 6.46. With the addition of the adsorbents, the solution pH changes. The initial pH of all the adsorbent systems is varied from 2 to 10 and the % removal at equilibrium is obtained as shown in Fig. 6. With all the adsorbents, it is found that the sorption of Se(IV) of decreases at alkaline pH and maximum removal is obtained at pH 2 to 3.

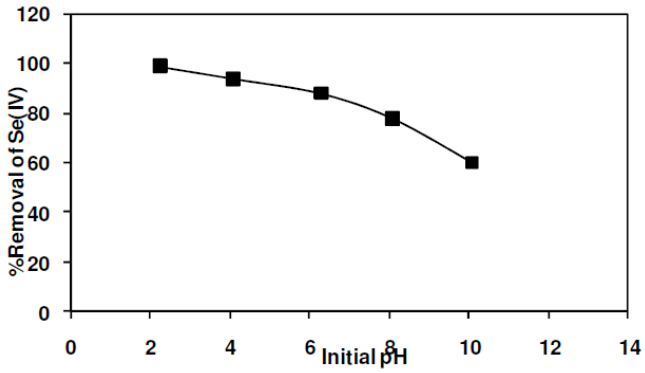

Fig. 6. Effect of initial pH on % Removal of Se(IV) by RHA. *T*=303K, C_o=100 µg/l.

Se(IV) species in aqueous solution include selenious acid (H_2SeO_3), biselenite ($HSeO_3^-$) and selenite(SeO_3^{2-}). Between pH 3.5 and 9.0, biselenite ion is the predominant ion in water. Above pH 9.0 selenite species dominates and as pH decreases below pH 3.5, selenious acid dominates. Se(IV) sorption decreases at alkaline pH due to the decrease of the fraction of the aqueous species of $HSeO_3^-$. For all systems, the final pH changes from its initial value of 6.46 to around 2.5.

Effect of Temperature

The effect of temperature on adsorption capacity of Se(IV) by $FeCl_3$ coated RHA is studied by carrying out from 293 to 323 K using different initial Se(IV) concentration at natural *pH* of the solutions. The equilibrium uptake of Se(IV) by different adsorbents were affected by temperature. It was indicated that the removal increased with increase in temperature. The increase in adsorption with the rise of temperature may be due to increase in swelling of the adsorbent allowing more active sites to become available for selenium. The optimum temperature for Se(IV) adsorption on RHA was found to be the 323 K within the temperature range studied.

3.3. Kinetic Study

The values of the pseudo-first-order adsorption rate constant k_f (Table 3) are determined using Eq. (1) by plotting $\log(q_e - q_t)$ against t for Se(IV) adsorption onto all the adsorbents with C_o=100 µg/l at 303 K for the first 30 minutes only.

Experimental results did not follow first-order kinetics given by as there was difference in two important aspects:

(i) $k_f(q_e - q_t)$ do not represent the number of available sites, and

(ii) log q_e was not equal to the intercept of the plot of $\log(q_e - q_t)$ against t.

Equation (2) has been fitted to the experimental data using a non-linear regression method to get the kinetic parameters of pseudo-second-order model. This has been accomplished by minimizing the respective coefficient of determination between experimental data and predicted values.

The best-fit values of h, q_e, and k_s along with the correlation coefficients for all the adsorbate–adsorbent systems and the optimum values of kinetic parameters are given in Table 3 for all the systems with C_o=100 μg/l used in the present study. The plot of the experimental adsorption capacity q_t with t is shown in Fig. 7.

Table 3. Kinetic Parameters for the Removal of Se(IV) by RHA for C_o=100 μg/l.

Pseudo 1st order equation	$q_t = q_e\left[1-\exp(-k_f t)\right]$
k_f (min^{-1})	0.0507
$q_{e,cal}$ (μg/g)	11.9788
$q_{e,exp}$ (μg/g)	14.6415
R^2	0.9516
Pseudo 2nd order equation	$q_t = \dfrac{tk_S q_e^2}{1+tk_S q_e}$
k_s (g/μg min)	0.0094
h (μg/g min)	2.1924
$q_{e,cal}$ (μg/g)	15.2674
R^2	0.9984
Weber Morris	$q_t = k_{id}\sqrt{t} + I$
K_{id1} (μg/g min)	2.0970
I_1 (μg/g)	0.7781
R_1^2	0.9427
K_{id2} (μg/g min)	0.2086
I_2 (μg/g)	12.0424
R_2^2	0.9616

The $q_{e,exp}$ and the $q_{e,cal}$ values for the pseudo-first-order model and pseudo-second-order models are also shown in Table 3. The $q_{e,exp}$ and the $q_{e,cal}$ values from the pseudo-second-order kinetic model are very close to each other. The calculated correlation coefficients are also closer to unity for pseudo-second-order kinetics than that for the pseudo first-order kinetic model. Therefore, the sorption can be approximated more appropriately by the pseudo-second-order kinetic model than the pseudo-first-order kinetic model for the adsorption of Se(IV) onto $FeCl_3$ coated RHA.

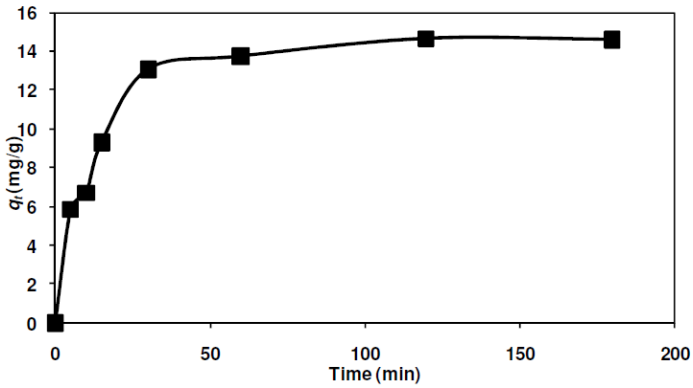

Fig. 7. Pseudo-Second-Order Kinetic Model for the Removal of Se(IV) by RHA at natural *pH*. *T*=303K, C_o=100µg/l.

Figure 8 represent plots of q_t versus $\sqrt{t}$ (equation 4) for the adsorption of Se(IV) onto $FeCl_3$ coated RHA to get Weber-Morris kinetic parameters. For all the systems with C_o=100 µg/l the data points represent bi-linear plots for the experimental data. The diffusion in the meso- and micro-pores is represented by the bi-linear plots for all systems shown in Fig. 8. The values of *I* (Table 3) give an idea about the thickness of the boundary layer, i.e., the larger the intercept, the greater is the boundary layer effect. The deviation of straight lines from the origin (Fig. 8) may be because of the difference between the rate of mass transfer in the initial and final stages of adsorption. Further, such deviation of straight line from the origin indicates that the pore diffusion is not the sole rate-controlling step. The values of k_{id} for C_o=100 µg/l as obtained from the slopes of the straight lines are listed in Table 3.

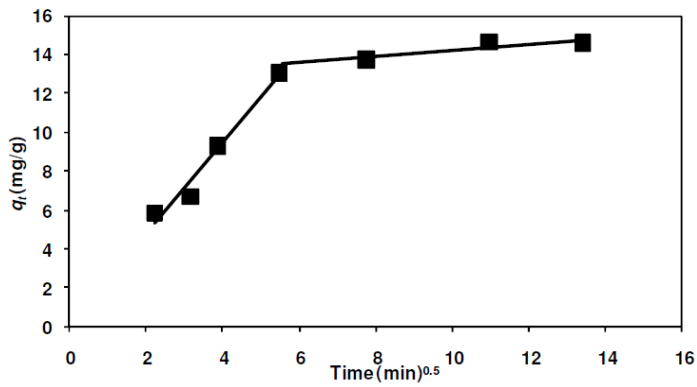

Fig. 8. Intra-Particle (Weber-Morris) Kinetic Model for the Adsorption of Se(IV) at Natural pH, Optimum Dosage and *T* = 303 K.

3.4. Equilibrium Study

The experimental equilibrium adsorption data of Se(IV) adsorption onto $FeCl_3$ coated RHA have been tested by using Freundlich, Langmuir, and Tempkin isotherm equations.

The Freundlich isotherm is valid for a heterogeneous adsorbent surface with a non-uniform distribution of heat of adsorption over the surface. The Langmuir isotherm, however, assumes that the sorption takes place at specific homogeneous sites within the adsorbent.

The parameters of the isotherm, and the correlation coefficient, R^2 for the fitting of the experimental data are listed in Table 4. By comparing the results of the values for the error functions and correlation coefficients, it was found that the Freundlich isotherm generally represent the equilibrium sorption of Se(IV) onto RHA.

Table 4. Isotherm Parameters and Error Functions for Se(IV) Adsorption onto RHA.

Freundlich					
Temp. (K)	K_F [(μg/g)/(μg/l)$^{1/n}$]	$1/n$	R^2	HYBRID	MPSD
293	3.392	0.805	0.9763	-1.0515	15.0579
303	3.603	0.751	0.9892	-0.0549	9.6165
313	4.547	0.667	0.9893	-0.5127	9.76114
323	4.045	0.662	0.9911	-0.3507	9.03912
Langmuir					
Temp. (K)	q_m (μg/g)	K_L (l/μg)	R^2	HYBRID	MPSD
293	283.54	0.0078	0.8165	0.77600161	13.78
303	224.98	0.0091	0.9264	1.06117	9.6165
313	168.98	0.0126	0.9699	-2.8651	8.9889
323	163.26	0.0108	0.9438	0.30968	10.845
Tempkin					
Temp. (K)	K_T (l/μg)	B_T	R^2	HYBRID	MPSD
293	0.1357	43.19	0.9791	-0.33	11.926
303	0.13258	38.92	0.9774	0.9499	13.072
313	0.14831	33.97	0.9831	1.4138	10.506
323	0.13037	32.34	0.9698	1.3579	16.379

3.5. Thermal Degradation of Spent Adsorbents

The spent adsorbents pose problems to their disposal and management. The recent trend emphasizes on utilizing them for some beneficial purpose and rendering them innocuous and benign to the environment before they are being disposed off. The use of low-cost adsorbents for the treatment of various wastewaters generates large volumes of solid waste. These solid wastes have great potential for energy recovery. However, the separation of the adsorbents from the solvents by sedimentation, filtration, centrifugation, dewatering and drying is very important. Se(IV) loaded adsorbents and blank adsorbents are studied for their thermal degradation characteristics by thermogravimetric (TG) instrument.

Thermal stability of RHA is directly dependent on the decomposition temperature of its various oxides and functional groups. The surface groups present on carbons and those formed as a result of interaction with oxidizing gases or solutions are generally quite stable even under vacuum at temperatures below 150°C, irrespective of the temperature at which they were formed. However, when the carbons are heated at higher temperatures, the surface groups decompose, producing CO (150-600°C), CO_2 (350-1000°C), water vapour and free hydrogen (500-1000°C). The principal experimental variables which could

affect the thermal degradation characteristics in air and nitrogen flow in a TG experiment are the pressure, the air (purge gas) flow rate, the heating rate and the weight of sample. In the present study, the operating pressure was kept slightly positive; the purge gas (air) and (nitrogen) flow rate was maintained at 200°C. The thermogravimetric analysis (TGA), differential thermal analysis (DTA) and differential thermo gravimetery (DTG) curves of the $FeCl_3$ coated and Se(IV) adsorbed RHA is shown in Figs. 9 and 10. Three different zones can be seen for the oxidizing atmosphere for all the blank and loaded adsorbent.

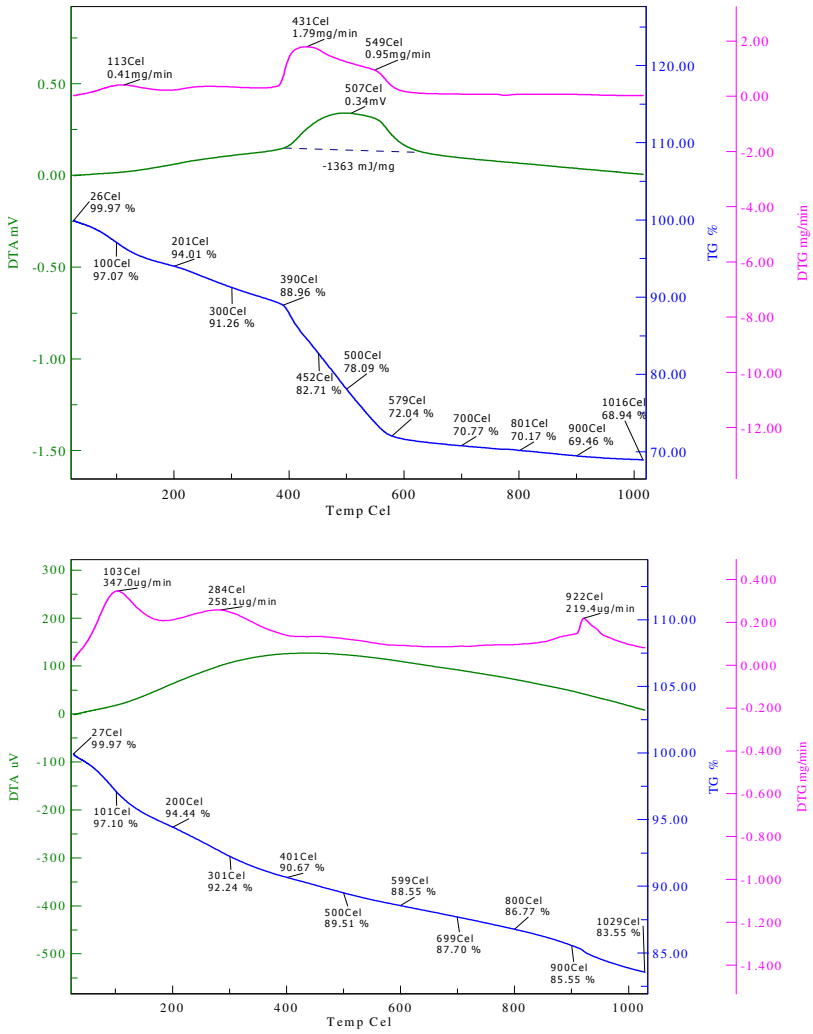

Fig. 9. TGA Analysis of
(a) Virgin and (b) Se(IV) Loaded RHA in Air Atmosphere.

To investigate the mechanism of Se(IV) adsorption as well as the role of porosity, the nature of interaction between Se(IV) and PAC was explored by thermo-gravimetric (TG) analysis under nitrogen and air atmospheres at a heating rate of 25 K/min. A peak in derivative thermogravimetric (DTG) curve at

temperature lower than 150°C (130-133°C) under both nitrogen and air atmospheres shows the removal of physisorbed water. Under nitrogen atmosphere, a somewhat steady weight loss with temperature is seen in TG curve.

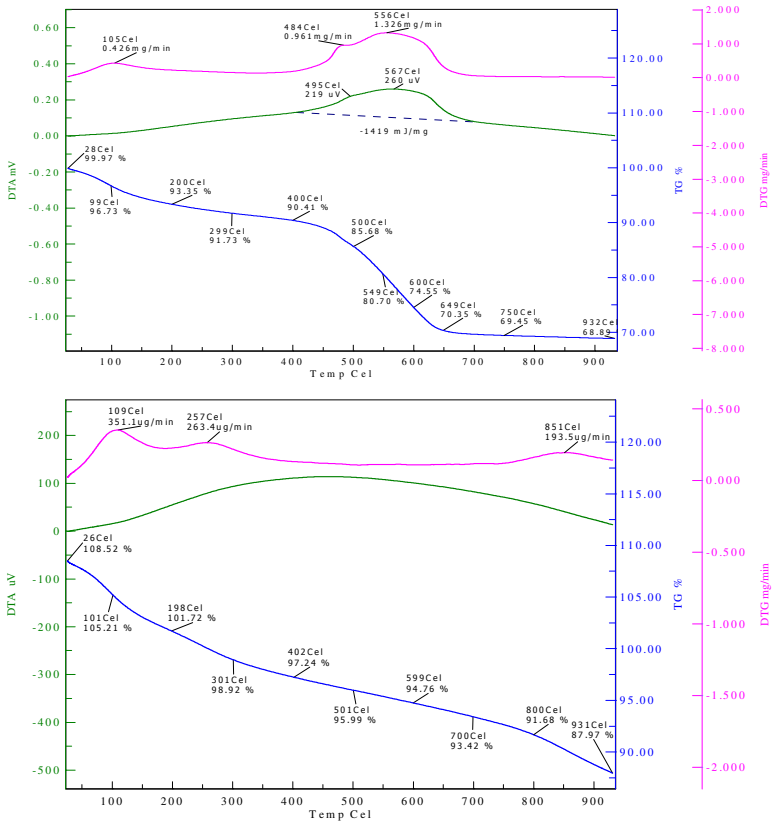

Fig. 10. TGA Analysis of
(a) Virgin and (b) Se(IV) Loaded RHA in Nitrogen Atmosphere.

The TG traces for the blank and Se(IV) loaded adsorbents show that the loss of moisture and the evolution of some lightweight molecules including water take place (6.62-16.1% weight loss in air atmosphere and 5.53 -17.83 weight loss in nitrogen atmosphere) from ambient temperature to < 200°C, for all the adsorbents. Higher temperature drying (> 100°C) occurs due to loss of the surface tension bound water of the particles. TG trace was also obtained for all the adsorbents, in which moisture and light volatile components loss (~31.03to 99.93% weight loss in air atmosphere and ~16.42 to 64.31% in the nitrogen atmosphere) takes place upto ~700°C for air and ~1000°C for nitrogen atmosphere. The distribution of volatiles released during thermal degradation and their characteristics along with DTA for blank and loaded adsorbents in an air and nitrogen atmosphere at a flow rate of 200 ml/min are presented in Tables 5 to 7.

Adsorbents (blank and loaded) show endothermic transition between room temperature and 200°C in the air and nitrogen atmosphere, indicating phase change during the heating process. The strong exothermic peak centered between 400-700

^{O}C is due to the oxidative degradation of the sample. This broad peak as that observed from the first derivative loss curve (DTG) as shown in Figs. 9 and 10 may be due to the combustion of carbon species. At higher temperatures (third zone), the samples present a gradual weight loss up to 950°C. This weight loss has been reported to be associated in part with the evolution of CO_2 and CO.

The maximum rate of weight loss in air atmosphere was obtained as 1.79 mg/min and in the nitrogen atmosphere 0.347 for RHA. The nature of the TG curve gives a clear indication that the two-step degradation is observed for RHA.

Table 5. Distribution of Volatiles Released during Thermal Degradation of Blank and Loaded Adsorbents in an Air and Nitrogen Atmosphere at a Flow Rate of 200 ml/min.

Adsorbent (Blank/ loaded)	%Weight loss in air atmosphere (approximate)				%Weight loss in nitrogen atmosphere (approximate)		%Total volatile matter including moisture in air	%Total volatile matter including moisture in nitrogen
	< 200°C	200-400°C	400-700°C	>700°C	<200°C	200-1000°C		
RHA	5.97	8	15.23	1.83	6.82	13.8	31.03	20.62
Se-RHA(Fe)	6.62	2.94	20.41	1.11	5.53	10.89	31.08	16.42

Table 6. Thermal Degradation Characteristics of Blank and Loaded Adsorbents in Air and Nitrogen Atmosphere at a Flow Rate of 200 ml/min.

Adsorbent (Blank/ loaded)	Air atmosphere					Nitrogen atmosphere				
	Drying range (°C)	Moisture (%)	Degradation range (°C)	T_{max} (°C)	Max. rate of weight loss (mg/min)	Drying range (°C)	Moisture (%)	Degradation range (°C)	T_{max} (°C)	Max. rate of weight loss (mg/min)
RHA	23-200	17.1	>200	431	1.79	26-200	3.31	>100	109	0.351
Se-RHA	28-195	2.9	>200	556	1.326	27-190	2.87	>200	103	0.357

Table 7. DTA for the Blank and Loaded Adsorbents in the Air and Nitrogen Atmosphere at Flow Rate 200 ml/min.

Adsorbent (Blank/ loaded)	Air atmosphere						Nitrogen atmosphere		
	ΔH_1 (MJ/kg)	T_{1i} (°C)	T_{2f} (°C)	ΔH_2 (MJ/kg)	T_{1i} (°C)	T_{2f} (°C)	ΔH (MJ/kg)	T_{1i} (°C)	T_{2f} (°C)
RHA	-	-	-	-1363	400	640	-	-	-
Se(IV)-RHA	-	-	-	-1419	410	760	-	-	-

4. Conclusions

On the basis of the studies and the results and discussion presented, the following conclusions were drawn:

- The FTIR spectra of the RHA indicated the presence of various types of functional groups, e.g., free and hydrogen bonded OH group, the silanol groups (Si-OH), alkenes, CO group stretching from aldehydes and ketones on the surface of adsorbents.
- Optimum RHA dosage is found to be 6 g/l for C_o=100 mg/l of Se(IV) removal.

- Percent removal of Se(IV) increases with the increase in adsorbent concentration, while removal per unit weight of adsorbent increases with the decrease in adsorbent concentration.
- Se(IV) adsorption onto RHA is high at low pH values, and decreased with the rise in initial pH.
- The sorption kinetics of Se(IV) onto RHA could be represented by the pseudo-second-order kinetic model.
- The adsorption processes could be well described by a two-stage diffusion model.
- Freundlich isotherms generally well represent the equilibrium adsorption of Se(IV) onto RHA.

References

1. Reill, C. (1996). *Selenium in Food and Health.* Blackie Academic and Professionals, London.
2. Ministry of Environment and Forests (2004). Status of water treatment plants in India. *Central Pollution Control Board Report* http://www.scribd.com/doc/13999104/WTPsStatusCPCB.
3. El-Shafey, E.I. (2007). Removal of Se(IV) from aqueous solution using sulphuric acid-treated peanut shell. *Journal of Environmental Management*, 84(4), 620–627.
4. Rovira, M.; Giménez, J.; Martínez, M.; Martínez-Lladó, X.; Joan de Pablo; Martí, V.; and Duro, L. (2008). Sorption of selenium(IV) and selenium(VI) onto natural iron oxides: Goethite and hematite. *Journal of Hazardous Materials*, 150(2), 279-284.
5. El-Shafey, E.I. (2007). Sorption of Cd(II) and Se(IV) from aqueous solution using modified rice husk. *Journal of Hazardous Materials,* 147(1-2), 546-555.
6. Peak, D. (2006). Adsorption mechanisms of selenium oxyanions at the aluminum oxide/water interface. *Journal of Colloid and Interface Science*, 303 (2), 337-345.
7. Sotiropoulos, A.K.; and Kamaratos, M. (2004) Selenium adsorption on Cs-covered Si(100) 2×1 surfaces. *Solid State Communications*, 129(10), 637-641.
8. Youwen, Y.; Vance, G.F.; Zhao, H. (2001) Selenium adsorption on Mg–Al and Zn–Al layered double hydroxides. *Applied Clay Science*, 20(1-2), 13-25.
9. U.S. Environmental Protection Agency (2001). *Selenium Treatment and Removal Alternatives: Demonstration Project*. Mine Waste Technology Program Activitiy III, Project 20. EPA/600/R-01/077.
10. Ohtake, A.; Komura, T.; Hanada, T.; Miwa, S.; Yasuda, T.; and Yao, T. (2000). Adsorption processes of Se on the GaAs (111)A - (2×2) surface. *Applied Surface Science*, 162-163, 419-424.
11. Dhillon, S.K.; and Dhillon, K.S. (1999). Adsorption-desorption reactions of selenium in some soils of India. *Geoderma*, 93(1-2), 19-31.
12. Kuan,W-H.; Shang, L.L.; Ming, K.W.; and Cheng, F.L. (1998). Removal of selenite (Se(IV)) and selenate (Se(VI)) by using Aluminum-Oxide-Coated sand. *Pregamon,* 32, 915-923.

13. Balistrieri, L.S.; and Chao, T.T. (1990). Adsorption of selenium by amorphous iron oxyhydroxide and manganese dioxide. *Geochimica et Cosmochimica Acta*, 54(3), 739-751.
14. Wasewar, K.L.; Prasad, B.; and Gulipalli, S.; (2009) Adsorption of selenium using bagasse fly ash (BFA), *CLEAN: Soil, Water, Air,* 37(7), 534-543.
15. Lagergren, S. (1898). About the theory of so called adsorption of solute substances. *Ksver Veterskapsakad Handl*, 24, 1-6.
16. Ho, Y.S.; and McKay, G. (1999). Pseudo-second-order model for sorption processes. *Process Biochemistry*, 34(5), 451-465.
17. Weber, W.J.; Asce, Jr J.M.; and Morris, J.C. (1963) Kinetics of adsorption on carbon from solutions. *Journal of Sanitary Engineering Division of American Society of Civil Engineering*, 89, 31-60.
18. Freundlich, H.M.F. (1906). Over the adsorption in solution. *Journal of Physics and Chemistry*, 57, 385-470.
19. Langmuir, I. (1918). The adsorption of gases on plane surfaces of glass, mica and platinum. *Journal of American. Chemical Society*, 40(9), 1361-1403.
20. Temkin, M.J.; and Pyzhev, V. (1940) Kinetics of ammonia synthesis on promoted iron catalysts. *Acta Physiochimica U.R.S.S.*, 12, 217-222.
21. Kapoor, A.; and Yang, R.T. (1989). Correlation of equilibrium. Adsorption data of condensible vapours on porous. Adsorbents. *Gas Separation and Purification*, 3(4), 187-192.
22. Marquardt, D.W. (1963). An algorithm for least-squares estimation of nonlinear parameters. *Journal of Society for Industrial Applications of Mathematics*, 11(2), 431-441.
23. Wasewar, K.L.; Kumar, S.; and Prasad, B. (2009). Adsorption of tin using granular activated carbon. *Journal of Environmental Protection Science*, 3, 41-52.
24. Wasewar, K.L.; Atif, M.; Prasad, B.; and Mishra, I.M. (2009). Batch adsorption of Zn using tea factory waste as an adsorbent. *Desalination*, 244(1-3), 66-71.
25. Wasewar, K.L.; Atif, M.; Prasad, B.; and Mishra, I.M. (2008). Adsorption of Zn using factory tea waste: kinetics, equilibrium and thermodynamics. *CLEAN: Soil, Water, Air,* 36(3), 320-329.
26. Dahlan, I.; Mei, G.M.; Kamaruddin, A.H.; Mohamed, A.; Lee, K.T. (2008). Removal of SO_2 and no over rice husk ash (rha)/cao-supported metal oxides. *Journal of Engineering Science & Technology* (*JESTEC*), 3(2), 109-116.
27. Tumin, N.D.; Chuah, A.L.; Zawani, Z.; Abdul Rashid, S. (2008). Adsorption of copper from aqueous solution by *elais guineensis* kernel activated carbon. *Journal of Engineering Science & Technology* (*JESTEC*), 3(2), 180-189.
28. Kumar, P.S.; and Gayathri, R. (2009). Adsorption of Pb^{2+} ions from aqueous solutions onto Bael tree leaf powder: isotherms, kinetics and thermodynamics. *Journal of Engineering Science & Technology* (*JESTEC*), 4(4), 381-399.
29. Rajoriya, R.K.; Prasad, B.; Mishra, I.M.; and Wasewar, K.L. (2007). Adsorption of benzaldehyde on granular activated carbon: kinetics, equilibrium, and thermodynamic. *Chemical and Biochemical Engineering*, 22(3), 219-226.
30. Wasewar, K.L.; Atif, M.; and Prasad, B. (2008). Characterization of factory tea waste as an adsorbent for removal of heavy metals. *Journal on Future Engineering and Technology*, 3(3), 47-53.
31. Wasewar, K.L.; Ravichandra, Y.; Kumar, M.A.; and Godbole, V. (2007). Adsorption mechanism for the adsorption of heavy metals using tea waste as an adsorbent. *Journal on Future Engineering and Technology*, 3(1), 41-46.